JLB

Article

Lack of the programmed death-1 receptor renders host susceptible to enteric microbial infection through impairing the production of the mucosal natural killer cell effector molecules

Shahram Solaymani-Mohammadi,[*,†,1] Omar Lakhdari,*[*] Ivelina Minev,*[*] Steve Shenouda,*[*] Blake F. Frey,[†] Rolf Billeskov,[†] Steven M. Singer,[‡] Jay A. Berzofsky,[†] Lars Eckmann,[§] and Martin F. Kagnoff*[*,2]

*Laboratory of Mucosal Immunology and [§]Department of Medicine, University of California, San Diego, La Jolla, California, USA; [†]Vaccine Branch, Center for Cancer Research, National Cancer Institute, National Institutes of Health, Bethesda, Maryland, USA; and [‡]Department of Biology and Center for Infectious Disease, Georgetown University, Washington, District of Columbia, USA

RECEIVED JANUARY 3, 2015; REVISED SEPTEMBER 12, 2015; ACCEPTED SEPTEMBER 25, 2015. DOI: 10.1189/jlb.4A0115-003RR

ABSTRACT

The programmed death-1 receptor is expressed on a wide range of immune effector cells, including T cells, natural killer T cells, dendritic cells, macrophages, and natural killer cells. In malignancies and chronic viral infections, increased expression of programmed death-1 by T cells is generally associated with a poor prognosis. However, its role in early host microbial defense at the intestinal mucosa is not well understood. We report that programmed death-1 expression is increased on conventional natural killer cells but not on CD4$^+$, CD8$^+$ or natural killer T cells, or CD11b$^+$ or CD11c$^+$ macrophages or dendritic cells after infection with the mouse pathogen *Citrobacter rodentium*. Mice genetically deficient in programmed death-1 or treated with anti–programmed death-1 antibody were more susceptible to acute enteric and systemic infection with *Citrobacter rodentium*. Wild-type but not programmed death-1–deficient mice infected with *Citrobacter rodentium* showed significantly increased expression of the conventional mucosal NK cell effector molecules granzyme B and perforin. In contrast, natural killer cells from programmed death-1–deficient mice had impaired expression of those mediators. Consistent with programmed death-1 being important for intracellular expression of natural killer cell effector molecules, mice depleted of natural killer cells and perforin-deficient mice manifested increased susceptibility to acute enteric infection with *Citrobacter rodentium*. Our findings suggest that increased programmed death-1 signaling pathway expression by conventional natural killer cells promotes host protection at the intestinal mucosa during acute infection with a bacterial gut pathogen by enhancing the expression and production of important effectors of natural killer cell function. *J. Leukoc. Biol.* 99: 475–482; 2016.

Introduction

The inhibitory receptor PD-1 (CD279) is expressed by T lymphocytes, macrophages, DCs, NK cells, and NKT cells [1–3]. The expression of PD-1 on T cells is increased in persistent viral infections and malignancies [1–3]. Moreover, studies have explored the role of PD-1 in the context of tumor surveillance and host defense against viral infections. Evidence has suggested that upregulation of PD-1 on virus-specific T cells contributes to T-cell exhaustion during persistent viral infections and that its increased expression is an indication of dysfunctional virus-specific T cells [4, 5]. In malignancies and persistent viral infections, increased PD-1 expression on immune effector cells has correlated positively with a poor prognosis [6]. Given the role of PD-1 in decreasing the immune responses in malignancies and chronic viral infections, efforts have been made to enhance the immune responses by inhibiting the PD-1 signaling pathway, with the aim of increasing the immune responses that might determine favorable clinical outcomes [7–9].

The intestinal mucosa is a major site of interaction between the host and enteric pathogens; however, limited evidence is available regarding the function of PD-1 during acute enteric infections. Furthermore, varying outcomes could be anticipated. Antibody blockade of the PD-1/PD-ligand 1 pathway, for example, resulted in enhanced levels of T-cell activation and facilitated production of IFN-γ in a mouse model of cerebral

Abbreviations: $^{-/-}$ = deficient, A/E = attaching-and-effacing, DC = dendritic cell, GrzB = granzyme B, LP = lamina propria, MLN = mesenteric lymph node, PD-1 = programmed death-1, p.i. = postinfection, WT = wild-type

The online version of this paper, found at www.jleukbio.org, *includes supplemental information.*

1. Correspondence: Vaccine Branch, Center for Cancer Research, National Cancer Institute, National Institutes of Health, Building 41, Room D702, Bethesda, Maryland 20892, USA. E-mail: shahram.sm@nih.gov

2. Deceased.

malaria caused by *Plasmodium berghei* [8]. In contrast, in an animal model of helminth infection, PD-1/PD-ligand 2 blockade enhanced Th2 immune responses during pulmonary infection with *Nippostrongylus brasiliensis* [10].

NK cells, a subset of lymphocytes of the innate immune system, have important roles in tumor surveillance and the control of viral infections [11]. NK cell activation and cytotoxicity are regulated by activating and inhibitory receptors that determine how resting NK cells sense microbial and non-microbial signals and control the NK cell effector function [11–13]. A lack of functional NK cells renders hosts susceptible to a wide range of viral, fungal, bacterial, and parasitic infections [14–16]. On recognition of their target cells, activated conventional NK cells secrete lytic proteins (e.g., GrzB and perforin) and cytokines (e.g., IFN-γ) [13, 17].

The murine intestinal pathogen *C. rodentium* has important virulence features in common with those of enteropathogenic *Escherichia coli* and enterohemorrhagic *E. coli* and, like those pathogens, forms A/E lesions on the apical surface of intestinal epithelial cells [18–21]. Innate and adaptive immune mechanisms have been proposed to determine the host resistance to and clearance of *C. rodentium* infection in mice. Mice lacking the cytokines IFN-γ [22, 23] and IL-12 [22] have greater susceptibility to infection and delayed clearance of *C. rodentium*. Likewise, mice defective in different components of the innate immune system (i.e., NK cells, DCs, murine cathelicidin-related antimicrobial peptide) manifest greater bacterial burdens in the initial days after infection with *C. rodentium* [20, 24, 25].

We report in the present study that PD-1$^{-/-}$ mice or mice treated with anti–PD-1 antibody have a phenotype characterized by a greater bacterial burden and systemic infection with *C. rodentium* in the early period after infection. Conventional NK cells from PD-1$^{-/-}$ mice challenged with *C. rodentium* in vivo manifest impaired intracellular expression of lytic proteins (i.e., GrzB and perforin). Thus, the lack of intact PD-1 signaling in conventional NK cells in the intestinal mucosa is paralleled by decreased, rather than increased, activation of NK-cell effector molecules during acute enteric bacterial infection.

MATERIALS AND METHODS

Mice

Sex- and age-matched WT C57BL/6J mice were purchased from Jackson Laboratory (Bar Harbor, ME, USA) or were bred at the University of California, San Diego, Animal Care Facility. Sex- and age-matched C57BL/6-Prf1tm1Sdz/J (perforin-deficient) mice were purchased from Jackson Laboratory. PD-1$^{-/-}$ mice on a C57BL/6J background were provided by Dr. William R. Green (Geisel School of Medicine at Dartmouth) with approval from Dr. Tasuku Honjo (Department of Immunology and Genomic Medicine, Kyoto University, Kyoto, Japan). All experiments used 6- to 8-week-old mice. Sex- and age-matched WT and PD-1$^{-/-}$ mice were cohoused for 1 wk before use at a 1:1 ratio. All experiments were performed in accordance with the guidelines approved by the University of California, San Diego, Institutional Animal Care and Use Committee, in compliance with the National Institutes of Health guidelines.

Infection protocol and quantification of bacterial burden

C. rodentium strain DBS100 (American Type Culture Collection 51459) was grown in Luria-Bertani broth at 37°C, harvested by centrifugation, and resuspended in PBS at a concentration of 5×10^9 CFU/ml. Mice were infected with 100 μl of the bacterial suspension containing 5×10^8 CFU of *C. rodentium* by oral gavage, as described previously [26]. For bacterial titrations, fecal pellets, collected at different times after infection, were weighed, homogenized in 2 ml of sterile PBS, serially diluted, and plated onto MacConkey agar (Difco; Difco Laboratories, Detroit, MI, USA). Liver, spleen, and MLNs were collected aseptically, weighed, and homogenized in 2 ml of sterile PBS. Serially diluted organ preparations were plated onto MacConkey agar plates. The plates were incubated overnight at 37°C, and the number of colonies was counted and expressed as CFU/g feces or CFU/g organ.

PD-1 blockade and depletion of NK cells in vivo

Rat anti-mouse PD-1 (clone RMP1–14), rat IgG_2a (clone 2A3), mouse anti-NK1.1 (clone PK136), and mouse IgG_2a (clone C1.18.4) were from Bioxcell (West Lebanon, NH, USA). For PD-1 blockade and NK-cell depletion, age- and sex-matched mice received intraperitoneal injections of 250 μg of blocking monoclonal antibodies or the corresponding isotype controls every other day during the entire course of infection, starting 4 d before *C. rodentium* oral inoculation.

Immunohistochemistry

The distal colons were opened longitudinally and washed in ice-cold PBS. Frozen tissues were fixed in optimal cutting temperature compound (Sakura Finetek, Torrance, CA, USA) and frozen in dry ice and 2-methylbutane. For *C. rodentium* staining, frozen tissues were cut and fixed in neutral buffered formalin for 10 min and blocked with TBST 3% BSA. The sections were incubated with a polyclonal rabbit antiserum (1:100) against the O152 LPS serotype (*E. coli* Poly 8; Denka Seiken, Tokyo, Japan), as described previously [19, 21, 27], followed by staining with a Cy3-conjugated donkey anti-rabbit IgG antibody (Jackson ImmunoReserach Laboratories, West Grove, PA, USA). F-actin filaments were visualized with Alexa Fluor 488 Phalloidin (1:400; Molecular Probe, Eugene, OR, USA). Hoechst (Life Technologies, Gaithersburg, MD, USA) was used at 1:10,000 for 10 min to visualize nuclei. Images from fluorescence microscopy were photographed using imaging software (PictureFrame; Optronics, Galeta, CA, USA). Digital images were processed using Adobe Photoshop, version 7.0 (Adobe Systems, San Jose, CA, USA).

Isolation of LP lymphocytes

The distal colon of uninfected or infected animals at day 3 p.i. were removed, cut longitudinally, and washed with ice-cold PBS. To remove epithelial cells, the colons were cut into small pieces and incubated for 10 min in predigestion solution (HBSS containing 5 mM EDTA, 10 mM HEPES, and 1 mM dithiothreitol supplemented with penicillin, streptomycin, and gentamicin) at 37°C with agitation. After incubation, the samples were shaken vigorously, supernatant was removed, and fresh predigestion solution was added to the tissue samples. Subsequently, the tissues were washed twice with ice-cold PBS, minced, and digested in DMEM (Sigma-Aldrich, St. Louis, MO, USA) containing 10% FBS, 420 μg/ml Liberase (Roche, Indianapolis, IN, USA), and 0.1 mg/ml DNase (Roche), supplemented with penicillin, streptomycin, and gentamicin, for 15 min at 37°C with gentle agitation. Digested tissues were passed through a 40-μm cell strainer (DB Falcon, San Jose, CA, USA), and isolated cells were washed with ice-cold PBS, counted, and stained with the indicated antibodies.

Tetramer staining for NKT cells

To evaluate the effects of anti-NK1.1 antibody on NKT cells, WT C57BL/6J mice were treated with anti-NK1.1 or isotype control (both from Bioxcell), as previously described. Single cells were isolated and stained with PE-labeled α-GalCer-CD1d tetramer (provided by the National Institutes of Health Core Facility, Atlanta, GA, USA) for 30 min at 4°C and subsequently stained for TCR-β at 4°C for 30 min and analyzed using an LSRII flow cytometer (BD Biosciences, San Diego, CA, USA).

Flow cytometry and intracellular staining

LP lymphocytes were isolated from the distal colon of uninfected or infected mice, as described previously. The MLNs and spleens from uninfected or infected mice were collected aseptically, and single-cell suspensions were

prepared by straining through a 70-μm nylon membrane (BD Falcon, San Jose, CA, USA). Red blood cells were lysed in cold isotonic NH_4Cl lysis buffer (155 mM NH_4Cl, 10 mM $KHCO_3$, and 100 mM EDTA, pH 7.4), and the remaining cells were washed twice with ice-cold PBS. The cells were incubated with 1 μg/10^6 cells anti-mouse CD16/CD32 (clone 93; Biolegend, San Diego, CA, USA) in FACS buffer (PBS supplemented with 3% FBS) for 15 min on ice to reduce nonspecific binding. Live/dead cell labeling was performed using a LIVE/DEAD Fixable Aqua Dead Cell Stain Kit (Life Technologies, Eugene, OR, USA) for 20 min at 4°C in the dark, according to the manufacturer's instructions. For surface staining, cells (~1.5–2 × 10^6) were directly stained in triplicate with cocktails of the following conjugated antibodies in FACS buffer: anti-CD3-BV421 (clone 17A2), anti-CD4-Alexa Fluor 488 (clone GK1.5), anti-CD8-Alexa Fluor 700 (clone 53-6.7), anti-NK1.1-APC (clone PK136; all from Biolegend), anti-CD49b-FITC (clone DX5), anti-CD11b-eFluor 450 (clone M1/70), anti-CD11c-Alexa Fluor 488 (clone N418), anti-PD-1-FITC (clone J43; all from eBioscience, San Diego, CA, USA), for 30 min at 4°C in the dark and were fixed using a Cytofix/Cytoperm kit (BD Biosciences) per the manufacturers' instructions. For intracellular staining, the cells were restimulated ex vivo for 8 h in the presence of PMA at 50 ng/ml and ionomycin at 750 ng/ml, adding Brefeldin A at 10 μg/ml (all from Sigma-Aldrich) for the last 6 h. The cells subsequently were fixed, permeabilized, and stained with cocktails of anti-perforin-PE (clone eBioOMAK-D) and anti-GrzB-PE-Cy7 (clone NGZB; all from eBioscience). Data were acquired using an LSRII flow cytometer (BD Bioscience) and were analyzed using FlowJo (Tree Star, Inc., San Carlos, CA, USA).

Histologic examination

The colon tissues were rinsed of fecal material with ice-cold PBS, rolled into a Swiss roll configuration, fixed in 10% buffered formalin, and subsequently embedded in paraffin. Tissue sections (5-μm thick) were deparaffinized in xylene, followed by hydration through graded ethanol solutions. The colon tissues were stained with H&E, and ≥20 full-length, well-oriented colon crypts were measured in each mouse.

Quantitative Real-Time PCR

Total RNA was extracted from the colons of uninfected and infected mice 3 d p.i. using TRIzol (Invitrogen, Carlsbad, CA, USA) and was reverse transcribed to cDNA using the iScript reverse transcription supermix (Bio-Rad, Hercules, CA, USA). SYBR Green based real-time quantitative PCR assays were performed using a StepOnePlus system (Applied Biosystems, Foster City, CA, USA). The primers used included *PD-1* forward: 5′-TTC AGG TTT ACC ACA AGC TGG-3′; *PD-1* reverse: 5′-TGA CAA TAG GAA ACC GGG AA-3′. Data were normalized according to the expression of the housekeeping gene *GAPDH*. *GAPDH* forward: 5′-CGA TGC CCC CAT GTT TGT GAT-3′; *GAPDH* reverse: 5′-GGT CAT GAG CCC CTT CCA CAA TGC-3′.

Statistical analysis

Data were analyzed using GraphPad Prism, version 6.07, software (GraphPad, San Diego, CA, USA) and expressed as the mean ± SEM. For statistical analyses, a 2-tailed Mann-Whitney *U* test or a Wilcoxon rank sum test was used, and $P < 0.05$ was considered statistically significant.

RESULTS

Lack of PD-1 impairs accumulation of NK cells in colon and is required for optimal effector function of NK cells under steady-state conditions

First, we compared the accumulation of NK cells in the colon LP using flow cytometry in naïve mice. PD-$1^{-/-}$ mice had a significantly lower percentage of NK cells compared with WT controls (**Fig. 1A**). Using intracellular staining, we next measured the effector function of NK cells in naïve mice, as demonstrated by intracellular expression of GrzB and perforin in the colon LP of PD-$1^{-/-}$ mice and WT controls. NK cells isolated from the colons of PD-$1^{-/-}$ mice had significantly fewer cells expressing either GrzB or perforin compared with the WT controls (Fig. 1B–D). These findings demonstrate that PD-1 is required for optimal production of the NK cell effector molecules (e.g., GrzB, perforin) under steady-state conditions.

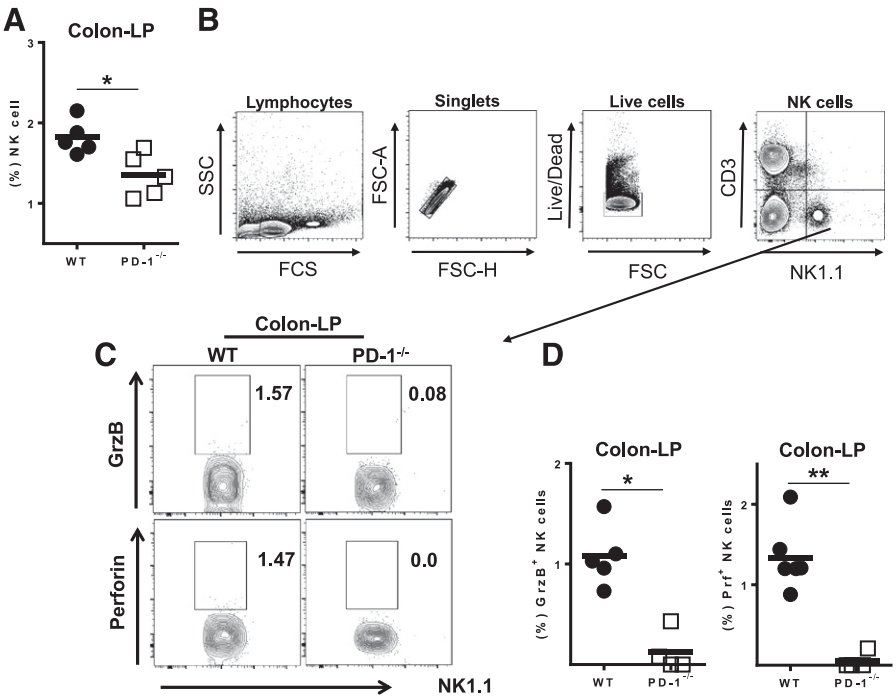

Figure 1. NK cell accumulation in the colon and the intracellular production of GrzB and perforin by colonic NK cells are impaired in the absence of intact PD-1. LP lymphocytes were isolated from sex- and age-matched naïve WT and PD-$1^{-/-}$ mice by enzymatic digestion. (A) Flow cytometric analysis of NK cells isolated from the colon LP of WT and PD-$1^{-/-}$. Data presented as mean and SEM, $n = 5$ mice per group. Data are representative of 2 independent experiments. (B) Gating strategy for flow cytometry analysis of NK cells defined as $CD3^-NK1.1^+$ cells. FSC and SSC represent forward and side scatter, respectively. (C) Intracellular expression of GrzB and perforin in WT (left) and PD-$1^{-/-}$ (right) mice. Data are representative of 3 pooled independent experiments ($n = 4$–5 mice per experiment). (D) Flow cytometric analysis of $NK1.1^+GrzB^+$ and $NK1.1^+$, perforin-positive cells isolated from colon LP. Fluorescence minus one controls were used to set the gates. Data are mean and SEM. *$P < 0.05$; **$P < 0.01$ (Mann-Whitney *U* test). Numbers indicate percentage of cells in each gate.

Increased susceptibility to enteric microbial infection in mice lacking PD-1

NK cells have been shown to play important roles in host defense against gut infections [15]. Considering the impaired accumulation of NK cells in the colon LP of naïve PD-1$^{-/-}$ mice compared with WT controls and the requirement of PD-1 for proper effector function of NK cells, we next hypothesized that PD-1$^{-/-}$ mice would show increased susceptibility to gut infection.

We used the murine pathogen *C. rodentium* to probe the function of PD-1 in mucosal microbial infection in the gut. PD-1$^{-/-}$ mice, compared with WT controls, had significantly higher bacterial numbers of *C. rodentium* in feces as early as day 3 p.i. (**Fig. 2A**). The increased *C. rodentium* infection in PD-1$^{-/-}$ mice was not due to a developmental abnormality in those mice, because similar results were found in adult WT mice treated with anti-PD-1 blocking antibody before infection (Fig. 2B and Supplemental Fig. 1). By day 3 p.i., significant numbers of translocated bacteria were present in the liver, spleen, and MLNs in PD-1$^{-/-}$ mice but not in the WT controls (**Fig. 3A**). Costaining for *C. rodentium* and actin in the distal colon of infected mice revealed that the distal colon surface epithelium of PD-1$^{-/-}$ mice was more densely covered with this A/E pathogen compared with the scattered bacteria associated with the epithelial surface in WT mice (Fig. 3B). *C. rodentium* was seen in small numbers within the LP of PD-1$^{-/-}$ mice but not WT mice. Likewise, WT mice treated with rat IgG_2a anti-PD-1 showed greater bacterial numbers in the liver, spleen, and MLNs compared with WT mice receiving control rat IgG_2a (Fig. 3C). However, anti-PD-1 therapy did not change the main bacterial taxa in the gut (i.e., Enterobacteriaceae, *Bacteroides, Prevotella, Porphyromonas, Enterococcus*, Actinobacteria). We also found that in the acute phase of *C. rodentium* infection, the mRNA transcripts for this pathogen were 10^4–10^5-fold higher than were other members of the Enterobacteriaceae family in the colon (data not shown). Immunolocalization of *C. rodentium* in the distal colon of WT mice treated with rat IgG_2a anti-PD-1 also showed that the intestinal epithelial surface was greatly covered with *C. rodentium*, but the WT mice receiving control rat IgG2a showed a lower bacterial burden after infection with an identical oral inocula (Fig. 3D). These findings suggest that PD-1 has an important role in early host defense mechanisms to this enteric infection.

PD-1 expression is upregulated after *C. rodentium* infection

C. rodentium infection significantly increased PD-1 mRNA expression in the colon mucosa of WT mice (**Fig. 4A**). We therefore characterized the mononuclear cell populations in the MLNs and spleen that manifested upregulated PD-1 expression after infection. Studies had demonstrated the importance of $CD4^+$ T cells and NK cells in the kinetics and clearance of C. *rodentium* infection [15, 22]. We found by flow cytometry an ~30% increase in the percentage of conventional NK cells (defined as $CD3^-NK1.1^+$), expressing PD-1 in the MLNs and spleen of infected mice by 3 d p.i. (Fig. 4B) but not by $CD3^+CD4^+$ or $CD3^+CD8^+$ T cells or by $CD11c^+$ or $CD11b^+$ mononuclear cells (i.e., putative DCs and macrophages,

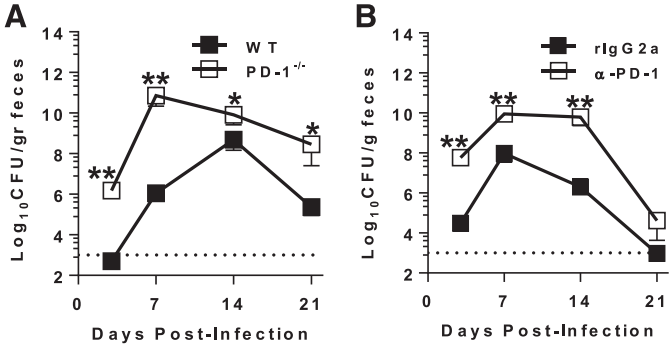

Figure 2. *C. rodentium* infection in PD-1$^{-/-}$ and anti-PD-1–treated mice. Sex- and age-matched mice (n = 5–7 per group) were infected with 5×10^8 CFU of *C. rodentium* by oral gavage. Fecal samples were collected at the indicated times after infection, and *C. rodentium* CFU/g feces was determined in WT C57BL/6J and PD-1$^{-/-}$ (A) and in WT mice (B) receiving either anti-PD-1 or isotype control antibody. Dotted lines represent the detection limit of the culture method. Data are representative of ≥3 independent experiments. Data are presented as mean ± SEM. $^*P < 0.05$; $^{**}P < 0.01$ (Mann-Whitney U test).

respectively) in those sites or the spleen (Supplemental Fig. 2). These findings suggest that PD-1 acting through conventional NK cells might contribute to early host defenses against *C. rodentium* infection.

Mice lacking conventional NK cells develop increased infection with *C. rodentium*

We tested whether the PD-1–dependent increase in the bacterial burden of *C. rodentium* was dependent on conventional NK cells by using an antibody against the surface marker NK1.1 (CD161) expressed by conventional NK cells. Analyses showed that the anti-NK1.1 antibody efficiently blocked conventional NK cells in WT mice when administered every other day (250 μg/mouse), starting 4 d before infection (**Fig. 5A** and **B**). Approximately 50–60% of NKT cells (defined as TCR-β^+CD1d-tetramer$^+$) also expressed NK1.1, and anti-NK1.1 administration did not completely deplete NKT cells (Supplemental Fig. 3). At 3 d after infection with *C. rodentium*, the mice treated with anti-NK1.1 had significantly greater numbers of *C. rodentium* in the feces than did those receiving control antibody (Fig. 5C). As shown in Fig. 5C, none of those mice receiving control mouse IgG_2a showed any translocated bacteria in the spleen. In contrast, *C. rodentium* was detected in the spleens of ~50% of mice receiving anti-NK1.1 at 3 d p.i. Likewise, immunolocalization of *C. rodentium* showed marked colonization of the distal colon in mice receiving anti-NK1.1 blocking antibody (Fig. 5D).

PD-1 is required for optimal GrzB and perforin production by conventional NK cells in the colon after *C. rodentium* infection

We analyzed the intracellular expression of GrzB and perforin by conventional NK cells using flow cytometry 3 d p.i. with *C. rodentium*. The intracellular expression of GrzB by conventional NK cells isolated from the LP of the colon (**Fig. 6A**) increased by more than twofold in response to *C. rodentium* infection. However, a lack of PD-1 significantly impaired the intracellular expression of GrzB by conventional NK cells in the colon at day 3 p.i. (**Fig. 6A**,

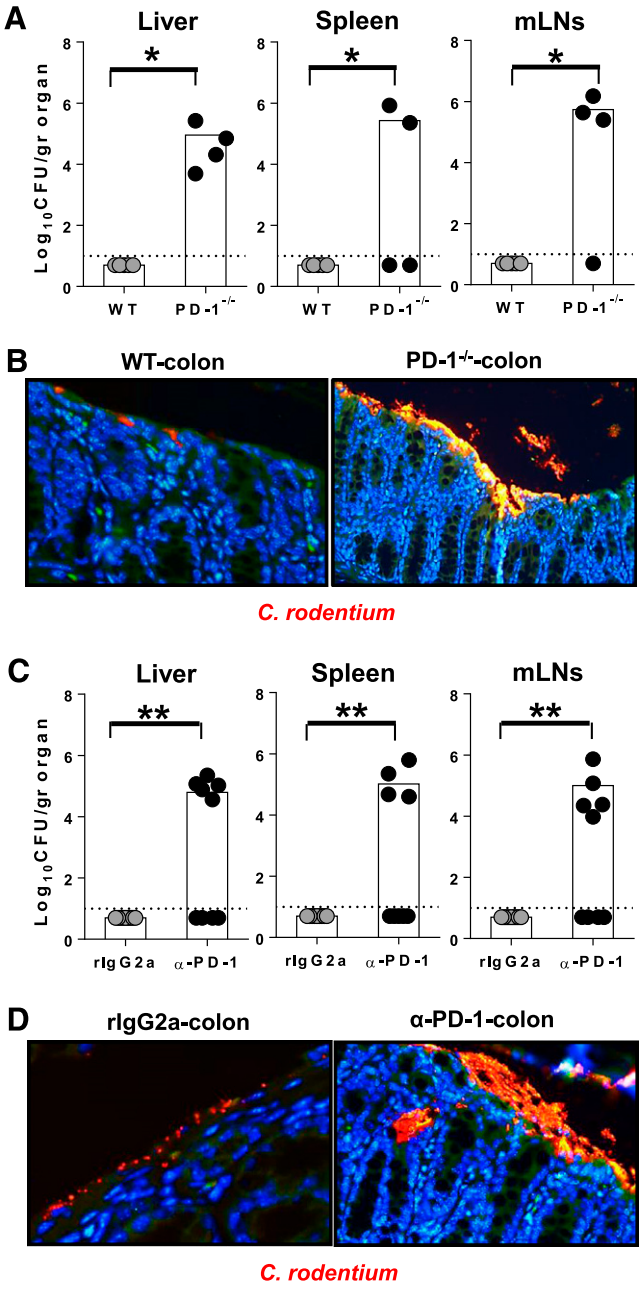

Figure 3. Systemic spread of intestinal infection with *C. rodentium* in PD-1$^{-/-}$ and WT mice treated with anti-PD-1. (A) Bacterial translocation into liver, spleen, and MLNs of infected WT and PD-1$^{-/-}$ mice were detected 3 d p.i ($n = 4$ mice per group). (B) Immunolocalization of *C. rodentium* in distal colon of WT and PD-1$^{-/-}$ mice. Actin filaments stained green, *C. rodentium* stained red, nuclei stained blue. (C) Bacterial translocation into liver, spleen, and MLNs of infected WT mice receiving control rat IgG$_{2a}$ (rIgG$_{2a}$) or rat IgG$_{2a}$ anti-PD-1 (α-PD-1) ($n = 9$ mice per group). (D) Immunolocalization of *C. rodentium* in distal colon of WT mice treated with control rIgG$_{2a}$ or α-PD-1. Similar data were obtained from 2 repeated experiments. Data are presented as mean ± SEM. $^*P < 0.05$; $^{**}P < 0.01$ (Mann-Whitney *U* test or Wilcoxon rank sum test).

left). Likewise, the percentage of perforin-expressing conventional NK cells (NK1.1$^+$, perforin-positive) isolated from LP of WT mice increased by more than threefold in response to gut infection at 3 d p.i. (Fig. 6B, left). Strikingly, the intracellular expression of perforin by conventional NK cells was impaired in the colon LP of PD-1$^{-/-}$ mice orally infected with *C. rodentium* compared with their WT counterparts at 3 d p.i. (Fig. 6B, right). However, no significant differences were observed in the intracellular expression of GrzB and perforin by CD8$^+$ T cells isolated from the colon LP of WT and PD-1$^{-/-}$ mice (data not shown).

Increased susceptibility to *C. rodentium* in perforin$^{-/-}$ mice

We hypothesized that impaired production of the cytotoxic effector perforin by conventional NK cells, alone or together with other conventional NK cell-effector molecules, could explain the increased susceptibility to *C. rodentium* in PD-1$^{-/-}$ mice. If perforin secreted by conventional NK cells contributed to the observed phenotype in PD-1$^{-/-}$ mice, mice lacking perforin would be predicted to display a phenotype resembling that of PD-1$^{-/-}$ mice after *C. rodentium* infection. Similar results to those in PD-1$^{-/-}$ mice were found 3 d p.i in perforin-deficient mice infected with *C. rodentium* (**Fig. 7A** and **B**).

DISCUSSION

PD-1 expressed by conventional NK cells in the intestinal mucosa had an important role in the early intestinal mucosal defense response against a prototypic A/E lesion-inducing murine intestinal pathogen. Expression of PD-1 in the colon of WT mice infected with *C. rodentium* was upregulated and restricted to conventional NK cells early after infection. PD-1 is known to function as a negative regulator of host immunity during chronic

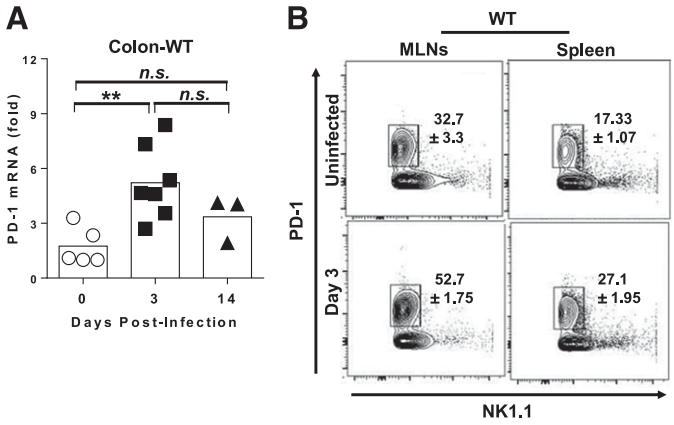

Figure 4. PD-1 expression in the colon increased after *C. rodentium* infection. (A) mRNA expression of PD-1 in distal colon of WT mice infected with 5×10^8 CFU of *C. rodentium* was measured at d 0 and 3 p.i. using RT-PCR. Data are presented as mean and SEM ($n = 3$–7 mice per group). Data are representative of 2 independent experiments. (B) Sex- and age-matched WT C57BL/6J mice ($n = 4$ per time point) were infected with 5×10^8 CFU of *C. rodentium* by oral gavage on d 0. MLNs and spleen were removed on d 0 and 3 p.i. PD-1 expressed on conventional NK cells (i.e., NK1.1$^+$CD3$^-$) from the MLNs and spleen was assessed by flow cytometry on d 0 and 3 p.i. Fluorescence minus one controls were used to set the gates. Numbers indicate percentage of NK1.1$^+$PD-1$^+$ cells. $^{**}P < 0.01$ (Mann-Whitney *U* test). Data are representative of 2 independent experiments ($n = 4$ mice per experiment). Numbers indicate percentage of cells in each gate.

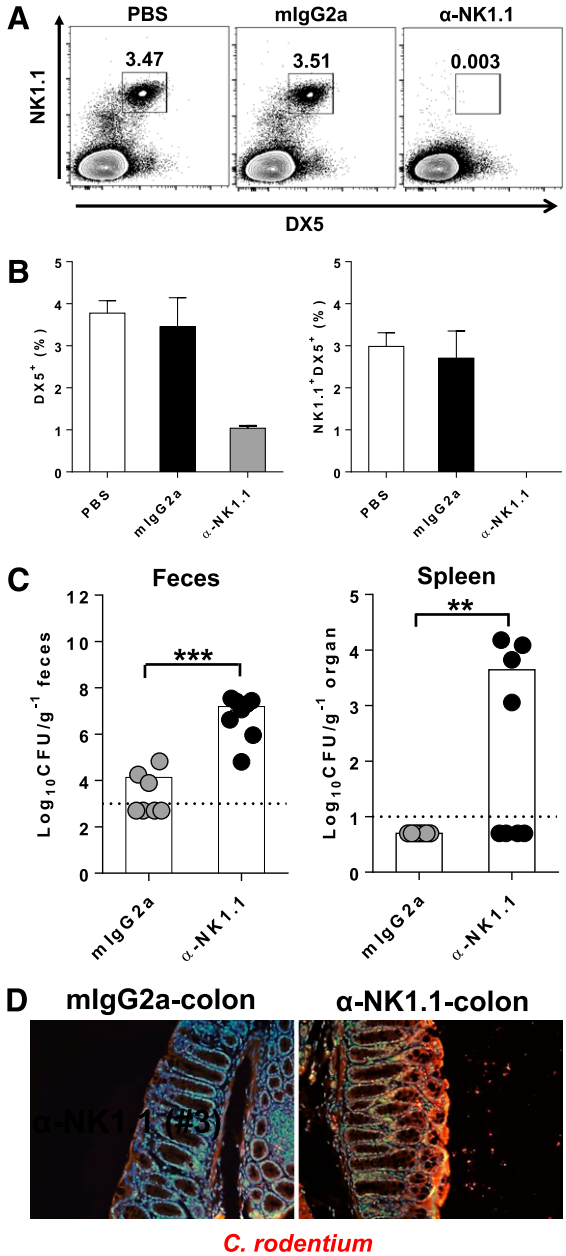

Figure 5. Increased *C. rodentium* infection in anti-NK1.1–treated mice. Efficacy of the α-NK1.1 antibody treatment in depleting NK cells in mice (A and B). Sex- and age-matched WT mice (n = 7–8 per group) receiving depleting anti-NK1.1 or mouse IgG_2a control were infected with 5×10^8 CFU of *C. rodentium* by oral gavage on d 0. Fecal samples and spleens were collected 3 d p.i., and *C. rodentium* CFU/g feces and spleen (C) were determined. Dotted lines indicate the detection limit of the culture method. (C) Immunostaining of *C. rodentium* in distal colon of WT mice receiving an anti-NK1.1 antibody or mouse IgG_2a control. $^{**}P < 0.01$; $^{***}P < 0.001$. Mann-Whitney U test (C, left) or Wilcoxon rank sum test (C, right). Data are presented as mean ± SEM.

infections with viruses, intracellular bacteria, and parasites [1, 2]. In addition to NK cells, PD-1 expression in persistent infections was increased on other innate and acquired immune effector cells (e.g., T cells, macrophages, NKT cells, and DCs), which was not the case for acute infection with *C. rodentium*. Moreover, it has been shown that targeting the PD-1 signaling pathway in mice using antibody to PD-1 or gene targeting of PD-1 enhances the immune responses against pathogens that cause persistent infections and results in improved resistance to infection [28, 29], rather than the decreased resistance seen during acute infection with *C. rodentium*.

NK cells have been reported to have a role in host defense to *C. rodentium* and several other enteric pathogens. However, the molecules, mediators, and mechanisms required for those responses are not known [15, 25, 30, 31]. By depleting conventional NK cells in vivo with specific antibody to NK1.1, we found that NK cells were relevant for host defense early in the course of *C. rodentium* infection [25]. We found that PD-1 was required for the optimal expression and production of effector molecules by conventional NK cells in *C. rodentium*-infected intestine. Mice deficient in PD-1 had an increased enteric microbial load and systemic infection with *C. rodentium* as early as 3 d after infection. In contrast, in WT controls, identical oral inocula resulted in infection largely confined to the luminal surface of the epithelial cells in the colon. Conventional NK cells present in the intestinal mucosa of PD-$1^{-/-}$ mice manifested abnormalities in the production of the lytic proteins GrzB and perforin.

Increased perforin production by mucosal NK cells from WT mice was restricted to the site of infection in the LP, suggesting the importance of local perforin production by NK cells in host resistance to this pathogen. Supporting this, perforin-deficient mice infected with *C. rodentium* had greater bacterial burdens with the pathogen in the feces at day 3 p.i. than did the WT controls, with a concomitant increased systemic infection, paralleling the phenotype of PD-$1^{-/-}$ mice.

NK cells can be activated during bacterial infections by proinflammatory cytokines [32]. However, direct activation of conventional NK cells by bacteria is less characterized [13], although some microbes were reported to contain cell wall–derived

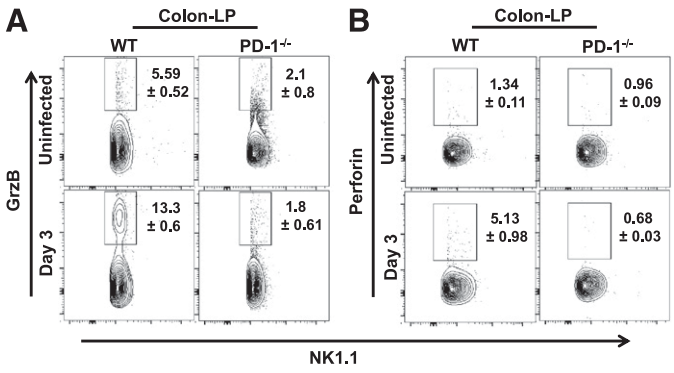

Figure 6. GrzB- and perforin-producing conventional NK cells in *C. rodentium* infected WT and PD-$1^{-/-}$ mice. Single cells from the colon LP of WT and PD-$1^{-/-}$ mice infected with 5×10^8 CFU of *C. rodentium* by oral gavage were isolated on d 0 and 3 p.i. and restimulated with PMA/ionomycin, as described previously. Flow cytometric analysis of intracellular expression of GrzB (A) and perforin (B) by conventional NK cells isolated from the colon LP of PD-$1^{-/-}$ and WT controls. Data are representative of 2 pooled independent experiments (n = 4–8 mice per experiment). Fluorescence minus one controls were used to set the gates. Numbers indicate the percentage of cells in each gate.

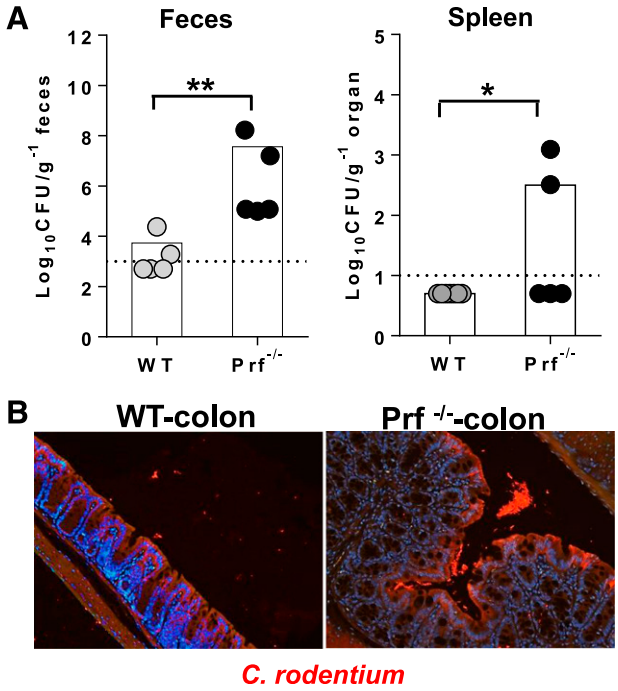

Figure 7. Increased susceptibility to *C. rodentium* in perforin-deficient ($Prf^{-/-}$) mice. Sex- and age-matched WT and $Prf^{-/-}$ mice ($n = 5$ per genotype) were infected with 5×10^8 CFU of *C. rodentium* by oral gavage on d 0. Fecal samples and spleens were collected 3 d p.i., and *C. rodentium* CFU/g feces and CFU/g spleen were determined (A). Dotted lines indicate the detection limit of the culture method. Data presented as mean ± SEM. $^*P < 0.05$; $^{**}P < 0.01$ (Mann-Whitney *U* test or Wilcoxon rank sum test). (B) Immunostaining of *C. rodentium* in distal colon of sex- and age-matched WT and $Prf^{-/-}$ mice infected with 5×10^8 CFU of *C. rodentium*. Data are representative of 2 independent experiments.

components that can bind to and activate conventional NK cells through NKp46 [13, 33]. Furthermore, it is known that NK cell lytic proteins and antimicrobial peptides mediate NK cell cytotoxicity against virus-infected cells and tumor cells [34] and that mice deficient in these factors are prone to infection with a wide variety of pathogens [35].

It is also known that conventional NK cells constitute an early source of IFN-γ after infection with intestinal pathogens such as *Salmonella typhimurium* [36]. We found that PD-1–deficient NK cells had decreased expression of IFN-γ. In contrast, *C. rodentium*–stimulated conventional NK cells from WT mice rapidly upregulated IFN-γ expression, suggesting possible direct simulation by *C. rodentium* or its products (data not shown). Furthermore, in WT mice, mucosal NK cells were the main source of IFN-γ 3 d after *C. rodentium* infection (data not shown). Taken together, these results are consistent with previous observations that conventional NK cells contribute a significant role in response to infection at mucosal surfaces by promptly upregulating the expression and secretion of IFN-γ [26, 37]. Others have reported that IFN-γ promotes the ultimate clearance of *C. rodentium* infection [22, 23].

Taken together, our results support the notion that PD-1 can determine host susceptibility to enteric bacterial infection by regulating the production of important effector molecules by NK cells. Because blocking PD-1 can render the host more susceptible to acute infection with enteric pathogens, in some clinical situations, this could represent an unanticipated consequence of PD-1 targeting therapies.

AUTHORSHIP

S.S.M. conceived the study, contributed hypotheses, designed the experiments, performed most of the experiments, analyzed the data, and wrote the manuscript. O.L. performed the real-time PCR, analyzed data, and contributed hypotheses. I.M. and S.S. conducted histologic examinations and performed confocal microscopy imaging and tissue staining. B.F.F. and R.B. performed NKT cell staining. S.M.S., L.E., and J.A.B. contributed hypotheses and analyzed data. M.F.K. conceived the experiments, contributed hypotheses, analyzed the data, and wrote the manuscript.

ACKNOWLEDGMENTS

This work was supported by the U.S. National Institutes of Health (NIH) National Institute of Diabetes and Digestive and Kidney Diseases Grant DK35108 (M.F.K), the NIH National Institute of Allergy and Infectious Diseases Grant AI 094492 (S.M.S), and by the NIH National Cancer Institute Intramural Research Program of the Center for Cancer Research (Project Z01-C04020; J.A.B). We are grateful to Dr. T. Honjo, Department of Immunology and Genomic Medicine, Kyoto University, Japan, and Dr. W.R. Green, the Geisel School of Medicine at Dartmouth for providing $PD\text{-}1^{-/-}$ mice. We thank E. Hanson, L. Hall, K. McKinnon, and L. Pasquet for technical assistance and C. McAllister and K. Vu for advice during the course of these studies.

DISCLOSURES

The authors declare no conflict of interest.

REFERENCES

1. Golden-Mason, L., Klarquist, J., Wahed, A. S., Rosen, H. R. (2008) Cutting edge: programmed death-1 expression is increased on immunocytes in chronic hepatitis C virus and predicts failure of response to antiviral therapy: race-dependent differences. *J. Immunol.* **180,** 3637–3641.
2. Yao, S., Wang, S., Zhu, Y., Luo, L., Zhu, G., Flies, S., Xu, H., Ruff, W., Broadwater, M., Choi, I. H., Tamada, K., Chen, L. (2009) PD-1 on dendritic cells impedes innate immunity against bacterial infection. *Blood* **113,** 5811–5818.
3. Norris, S., Coleman, A., Kuri-Cervantes, L., Bower, M., Nelson, M., Goodier, M. R. (2012) PD-1 expression on natural killer cells and CD8(+) T cells during chronic HIV-1 infection. *Viral Immunol.* **25,** 329–332.
4. Dyavar Shetty, R., Velu, V., Titanji, K., Bosinger, S. E., Freeman, G. J., Silvestri, G., Amara, R. R. (2012) PD-1 blockade during chronic SIV infection reduces hyperimmune activation and microbial translocation in rhesus macaques. *J. Clin. Invest.* **122,** 1712–1716.
5. Dietze, K. K., Zelinskyy, G., Liu, J., Kretzmer, F., Schimmer, S., Dittmer, U. (2013) Combining regulatory T cell depletion and inhibitory receptor blockade improves reactivation of exhausted virus-specific $CD8^+$ T cells and efficiently reduces chronic retroviral loads. *PLoS Pathog.* **9,** e1003798.
6. Duraiswamy, J., Freeman, G. J., Coukos, G. (2013) Therapeutic PD-1 pathway blockade augments with other modalities of immunotherapy T-cell function to prevent immune decline in ovarian cancer. *Cancer Res.* **73,** 6900–6912.
7. Butler, N. S., Moebius, J., Pewe, L. L., Traore, B., Doumbo, O. K., Tygrett, L. T., Waldschmidt, T. J., Crompton, P. D., Harty, J. T. (2011) Therapeutic blockade of PD-L1 and LAG-3 rapidly clears established blood-stage *Plasmodium* infection. *Nat. Immunol.* **13,** 188–195.
8. Hafalla, J. C., Claser, C., Couper, K. N., Grau, G. E., Renia, L., de Souza, J. B., Riley, E. M. (2012) The CTLA-4 and PD-1/PD-L1 inhibitory

pathways independently regulate host resistance to Plasmodium-induced acute immune pathology. *PLoS Pathog.* **8,** e1002504.
9. Velu, V., Titanji, K., Zhu, B., Husain, S., Pladevega, A., Lai, L., Vanderford, T. H., Chennareddi, L., Silvestri, G., Freeman, G. J., Ahmed, R., Amara, R. R. (2009) Enhancing SIV-specific immunity in vivo by PD-1 blockade. *Nature* **458,** 206–210.
10. Huber, S., Hoffmann, R., Muskens, F., Voehringer, D. (2010) Alternatively activated macrophages inhibit T-cell proliferation by Stat6-dependent expression of PD-L2. *Blood* **116,** 3311–3320.
11. Vivier, E., Tomasello, E., Baratin, M., Walzer, T., Ugolini, S. (2008) Functions of natural killer cells. *Nat. Immunol.* **9,** 503–510.
12. Bryceson, Y. T., March, M. E., Barber, D. F., Ljunggren, H. G., Long, E. O. (2005) Cytolytic granule polarization and degranulation controlled by different receptors in resting NK cells. *J. Exp. Med.* **202,** 1001–1012.
13. Horowitz, A., Stegmann, K. A., Riley, E. M. (2011) Activation of natural killer cells during microbial infections. *Front. Immunol.* **2,** 88.
14. Sirén, J., Sareneva, T., Pirhonen, J., Strengell, M., Veckman, V., Julkunen, I., Matikainen, S. (2004) Cytokine and contact-dependent activation of natural killer cells by influenza A or Sendai virus-infected macrophages. *J. Gen. Virol.* **85,** 2357–2364.
15. Hall, L. J., Murphy, C. T., Hurley, G., Quinlan, A., Shanahan, F., Nally, K., Melgar, S. (2013) Natural killer cells protect against mucosal and systemic infection with the enteric pathogen *Citrobacter rodentium*. *Infect. Immun.* **81,** 460–469.
16. Chen, Q., Amaladoss, A., Ye, W., Liu, M., Dummler, S., Kong, F., Wong, L. H., Loo, H. L., Loh, E., Tan, S. Q., Tan, T. C., Chang, K. T., Dao, M., Suresh, S., Preiser, P. R., Chen, J. (2014) Human natural killer cells control *Plasmodium falciparum* infection by eliminating infected red blood cells. *Proc. Natl. Acad. Sci. USA* **111,** 1479–1484.
17. Cooper, M. A., Fehniger, T. A., Fuchs, A., Colonna, M., Caligiuri, M. A. (2004) NK cell and DC interactions. *Trends Immunol.* **25,** 47–52.
18. Zheng, Y., Valdez, P. A., Danilenko, D. M., Hu, Y., Sa, S. M., Gong, Q., Abbas, A. R., Modrusan, Z., Ghilardi, N., de Sauvage, F. J., Ouyang, W. (2008) Interleukin-22 mediates early host defense against attaching and effacing bacterial pathogens. *Nat. Med.* **14,** 282–289.
19. Vallance, B. A., Deng, W., Knodler, L. A., Finlay, B. B. (2002) Mice lacking T and B lymphocytes develop transient colitis and crypt hyperplasia yet suffer impaired bacterial clearance during *Citrobacter rodentium* infection. *Infect. Immun.* **70,** 2070–2081.
20. Iimura, M., Gallo, R. L., Hase, K., Miyamoto, Y., Eckmann, L., Kagnoff, M. F. (2005) Cathelicidin mediates innate intestinal defense against colonization with epithelial adherent bacterial pathogens. *J. Immunol.* **174,** 4901–4907.
21. Khan, M. A., Ma, C., Knodler, L. A., Valdez, Y., Rosenberger, C. M., Deng, W., Finlay, B. B., Vallance, B. A. (2006) Toll-like receptor 4 contributes to colitis development but not to host defense during *Citrobacter rodentium* infection in mice. *Infect. Immun.* **74,** 2522–2536.
22. Simmons, C. P., Goncalves, N. S., Ghaem-Maghami, M., Bajaj-Elliott, M., Clare, S., Neves, B., Frankel, G., Dougan, G., MacDonald, T. T. (2002) Impaired resistance and enhanced pathology during infection with a noninvasive, attaching-effacing enteric bacterial pathogen, *Citrobacter rodentium*, in mice lacking IL-12 or IFN-gamma. *J. Immunol.* **168,** 1804–1812.
23. Shiomi, H., Masuda, A., Nishiumi, S., Nishida, M., Takagawa, T., Shiomi, Y., Kutsumi, H., Blumberg, R. S., Azuma, T., Yoshida, M. (2010) Gamma interferon produced by antigen-specific $CD4^+$ T cells regulates the mucosal immune responses to *Citrobacter rodentium* infection. *Infect. Immun.* **78,** 2653–2666.
24. Hirata, Y., Egea, L., Dann, S. M., Eckmann, L., Kagnoff, M. F. (2010) GM-CSF-facilitated dendritic cell recruitment and survival govern the intestinal mucosal response to a mouse enteric bacterial pathogen. *Cell Host Microbe* **7,** 151–163.
25. Reid-Yu, S. A., Small, C. L., Coombes, B. K. (2013) $CD3^-NK1.1^+$ cells aid in the early induction of a Th1 response to an attaching and effacing enteric pathogen. *Eur. J. Immunol.* **43,** 2638–2649.
26. Maaser, C., Housley, M. P., Iimura, M., Smith, J. R., Vallance, B. A., Finlay, B. B., Schreiber, J. R., Varki, N. M., Kagnoff, M. F., Eckmann, L. (2004) Clearance of *Citrobacter rodentium* requires B cells but not secretory immunoglobulin A (IgA) or IgM antibodies. *Infect. Immun.* **72,** 3315–3324.
27. Bergstrom, K. S., Kissoon-Singh, V., Gibson, D. L., Ma, C., Montero, M., Sham, H. P., Ryz, N., Huang, T., Velcich, A., Finlay, B. B., Chadee, K., Vallance, B. A. (2010) Muc2 protects against lethal infectious colitis by disassociating pathogenic and commensal bacteria from the colonic mucosa. *PLoS Pathog.* **6,** e1000902.
28. Zander, R. A., Obeng-Adjei, N., Guthmiller, J. J., Kulu, D. I., Li, J., Ongoiba, A., Traore, B., Crompton, P. D., Butler, N. S. (2015) PD-1 co-inhibitory and OX40 co-stimulatory crosstalk regulates helper T cell differentiation and anti-*Plasmodium* humoral immunity. *Cell Host Microbe* **17,** 628–641.
29. McNab, F. W., Berry, M. P., Graham, C. M., Bloch, S. A., Oni, T., Wilkinson, K. A., Wilkinson, R. J., Kon, O. M., Banchereau, J., Chaussabel, D., O'Garra, A. (2011) Programmed death ligand 1 is over-expressed by neutrophils in the blood of patients with active tuberculosis. *Eur. J. Immunol.* **41,** 1941–1947.
30. Dann, S. M., Wang, H. C., Gambarin, K. J., Actor, J. K., Robinson, P., Lewis, D. E., Caillat-Zucman, S., White, A. C., Jr. (2005) Interleukin-15 activates human natural killer cells to clear the intestinal protozoan *cryptosporidium*. *J. Infect. Dis.* **192,** 1294–1302.
31. Sotolongo, J., Kanagavelu, S., Hyun, J., Ruiz, J., Fukata, M. (2012) TRIF mobilizes unique primary defense against gram-negative bacteria in intestinal interface. *Gut Microbes* **3,** 437–441.
32. Sivori, S., Falco, M., Della Chiesa, M., Carlomagno, S., Vitale, M., Moretta, L., Moretta, A. (2004) CpG and double-stranded RNA trigger human NK cells by Toll-like receptors: induction of cytokine release and cytotoxicity against tumors and dendritic cells. *Proc. Natl. Acad. Sci. USA* **101,** 10116–10121.
33. Esin, S., Batoni, G., Counoupas, C., Stringaro, A., Brancatisano, F. L., Colone, M., Maisetta, G., Florio, W., Arancia, G., Campa, M. (2008) Direct binding of human NK cell natural cytotoxicity receptor NKp44 to the surfaces of mycobacteria and other bacteria. *Infect. Immun.* **76,** 1719–1727.
34. Lodoen, M. B., Lanier, L. L. (2006) Natural killer cells as an initial defense against pathogens. *Curr. Opin. Immunol.* **18,** 391–398.
35. Schmidt, S., Tramsen, L., Hanisch, M., Latgé, J. P., Huenecke, S., Koehl, U., Lehrnbecher, T. (2011) Human natural killer cells exhibit direct activity against *Aspergillus fumigatus* hyphae, but not against resting conidia. *J. Infect. Dis.* **203,** 430–435.
36. Harrington, L., Srikanth, C. V., Antony, R., Shi, H. N., Cherayil, B. J. (2007) A role for natural killer cells in intestinal inflammation caused by infection with *Salmonella enterica* serovar Typhimurium. *FEMS Immunol. Med. Microbiol.* **51,** 372–380.
37. Barakat, F. M., McDonald, V., Di Santo, J. P., Korbel, D. S. (2009) Roles for NK cells and an NK cell-independent source of intestinal gamma interferon for innate immunity to *Cryptosporidium parvum* infection. *Infect. Immun.* **77,** 5044–5049.

KEY WORDS:
Citrobacter rodentium · granzyme B · perforin · attaching/effacing bacteria · PD-1